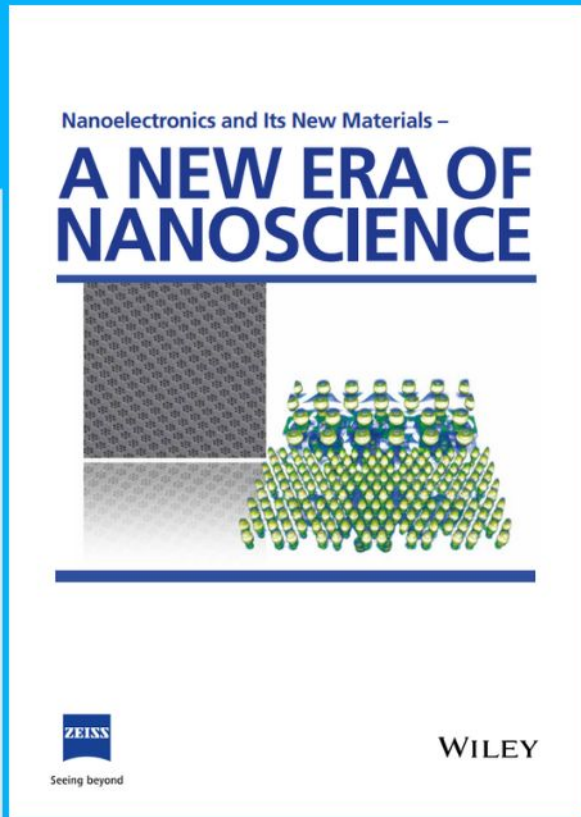




Nanoelectronics and Its New Materials – A NEW ERA OF NANOSCIENCE



Discover the recent advances in electronics research and fundamental nanoscience.

Nanotechnology has become the driving force behind breakthroughs in engineering, materials science, physics, chemistry, and biological sciences. In this compendium, we delve into a wide range of novel applications that highlight recent advances in electronics research and fundamental nanoscience. From surface analysis and defect detection to tailored optical functionality and transparent nanowire electrodes, this eBook covers key topics that will revolutionize the future of electronics.

To get your hands on this valuable resource and unleash the power of nanotechnology, simply download the eBook now. Stay ahead of the curve and embrace the future of electronics with nanoscience as your guide.



Seeing beyond

WILEY

Actuating Supramolecular Shape Memorized Hydrogel Toward Programmable Shape Deformation

Huanhuan Lu, Baoyi Wu, Xuxu Yang, Jiawei Zhang,* Yukun Jian, Huizhen Yan, Dachuan Zhang, Qunji Xue, and Tao Chen*

Inspired by nature, diverse biomimetic hydrogel actuators are fabricated and become one of the most essential components of bionics research. Usually, the anisotropic structure of a hydrogel actuator is generated at the early fabrication process, only a specific shape transformation behavior can be produced under external stimuli, and thus has limited the development of hydrogel actuators toward the biomimetic shape deformation behavior. Herein, a novel bilayer hydrogel having a thermoresponsive actuating layer and a metal ion-responsive memorizing layer is proposed, therefore, a 2D hydrogel film can be fixed into various 3D shapes via supramolecular metal-ligand coordination, with further realizing programmable 4D shape deformation under the stimulus of temperature. By manipulating the temporary shapes via shape memory behavior, various temporary anisotropic structures can be obtained via the bilayer hydrogel, thus producing diverse reversible shape deformation performances, which is expected to promote the development of intelligent polymeric materials.

materials in the rising area of intelligent research,^[6,7] have aroused increasing interest and shown promising applications in the fields of soft robotics,^[8,9] biomedical engineering,^[10–12] and biomimetic manufacturing.^[13] In the past decade, simple bending, folding, and complex shape deformations have been achieved by inducing anisotropic structure such as gradient,^[14,15] bilayer,^[16,17] patterned,^[18–20] or orient structure^[21,22] in hydrogel. For example, Wu et al. have proposed a novel strategy to achieve planar-to-helical 3D shape deformation by patterning on the surface of hydrogel sheet.^[23] Recently, Hsia et al. proved that hydrogel actuators with different original shapes (aspect ratios or shape) may produce different deformations.^[24] In order to better control the anisotropic structure of hydrogel

1. Introduction

Nature is considered as the common source of inspiration in both designing and fabricating of intelligent materials.^[1–5] Smart hydrogel actuators, one of the most anticipated

actuators, biomimetic 4D printing was introduced as a new concept to realize complex shape transformation.^[25–30] However, both the anisotropic structure and original shape of hydrogel actuators are normally determined at the early fabrication process and cannot be changed afterward, therefore, a hydrogel actuator usually could only produce a specific shape deformation behavior.

In addition to the above method, to achieve various shape deformation from one hydrogel actuator, another promising intelligent polymeric materials, supramolecular shape memory hydrogels^[31–33] have been considered because they could be stabilized into various temporary shapes via reversible molecular switches including hydrogen bonds,^[34,35] host–guest interaction,^[36] metal–ligand coordination,^[37] and so on. It can be anticipated that if a memorizing system is introduced into hydrogel actuator, the anisotropic structure of hydrogel could be altered optionally through the shape fixation process, and the temporary anisotropic structure could be erased during the shape recovery process, therefore various shape deformation performances could be generated by one specific hydrogel actuator.

Herein, we present a bilayer hydrogel that is composed of a thermoresponsive actuating layer and a metal ion-responsive memorizing layer to achieve programmable 4D shape deformation. In this system, a 2D hydrogel film can be fixed into various 3D shapes via supramolecular metal–ligand coordination, with further realizing programmable 4D shape deformation under the stimulus of temperature. By manipulating the temporary shapes via shape memory behavior, various temporary anisotropic structures could be obtained via actuating the


H. Lu, B. Wu, Prof. J. Zhang, Y. Jian, H. Yan, D. Zhang, Prof. Q. Xue, Prof. T. Chen
Key Laboratory of Marine Materials and Related Technologies
Zhejiang Key Laboratory of Marine Materials and Protective Technologies

Ningbo Institute of Material Technology and Engineering
Chinese Academy of Sciences
Ningbo 315201, P. R. China
E-mail: zhangjiawei@nimte.ac.cn; tao.chen@nimte.ac.cn

H. Lu, B. Wu, Prof. J. Zhang, Y. Jian, Prof. Q. Xue, Prof. T. Chen
School of Chemical Sciences
University of Chinese Academy of Sciences
19A Yuquan Road, Beijing 100049, P. R. China

Dr. X. Yang
Department of Engineering Mechanics and Center for X-Mechanics
Zhejiang University
Hangzhou 310027, P. R. China

H. Yan
Department of Polymer Materials
College of Materials Science and Engineering
Shanghai University
Nanchen Road 333, Shanghai 200444, P. R. China

 The ORCID identification number(s) for the author(s) of this article can be found under <https://doi.org/10.1002/smll.202005461>.

DOI: 10.1002/smll.202005461

bilayer hydrogel, thus producing diverse reversible shape deformation performances.

The bilayer hydrogel was prepared by two-step photopolymerization. An alginate/polyacrylamide (Alg/PAAm) semi-interpenetrating hydrogel was polymerized first under UV irradiation as the shape memorizing layer, then a thermoresponsive poly(*N*-isopropylacrylamid) (PNIPAm) actuating layer was fabricated on the top of the memorizing layer (Scheme S1, Supporting Information). The morphology of the Alg/PAAm-PNIPAm bilayer hydrogel was explored by scanning electronic microscopy (SEM). As shown in Figure S1, Supporting Information and Figure 1b II, two porous layers are firmly connected by a dense interfacial layer with a width of about 30 μm , which is probably because PNIPAm solution would penetrate into the top of the Alg/PAAm layer before the formation of the PNIPAm layer. In traditional actuating process, a bilayer hydrogel would transform from sheet to spherical or from straight to arc under the trigger of heat because of the shrinkage of the PNIPAm layer (Figure 1a,b I; Figures S2 and S3, Supporting Information). Due to the interactions between metal ions and alginate chains, when the wings of butterfly shaped bilayer hydrogel were deformed into a curved shape and exposed to metal ions, the metal ion-Alg interactions would form and serve as temporary crosslinks to stabilize the deformed shape (Figure 1a,b III). The shape fixity ratio was explored to determine the shape memory function of bilayer hydrogel, and the shape fixity ratio generated by trivalent metal ions is generally higher than that generated by divalent metal ions (Figure 1b IV), which is because of the binding constants between alginate and trivalent metal ions are usually larger than that with divalent metal ions.^[38,39]

and the shape fixity ratio can reach 100% if the bilayer hydrogel was treated by Fe^{3+} . Then when the temperature exceeds the phase transition temperature of the PNIPAm layer, the PNIPAm layer would shrink and the wings of butterfly-shaped bilayer hydrogel would transform starting from the temporary shape into soaring shaped (Figure 1a). Besides, both the memorizing and actuating processes were reversible, the soaring shaped hydrogel would transform into curved shape in cold water, and the temporary anisotropic structure could be erased by EDTA and the hydrogel would return to its original shape (Figure 1a). By integrating shape memory function into hydrogel actuator, we present a general approach to fabricate hydrogel actuators with diverse complex shape transformation behaviors, which would inspire the design and fabrication of novel intelligent polymeric materials.

2. Results and Discussion

The shape memory function of the bilayer hydrogels was explored at first. A bilayer hydrogel strip is manually bent toward the memorizing layer, and then immersed into the solution of metal ions, metal ions would diffuse into the hydrogel and crosslink the alginate chains in the memorizing layer, the metal ion-Alg coordination would serve as reversible molecular switches to fix the deformed shape (Figure 2a). The shape fixity ratio was calculated according to previous reports.^[40] In order to investigate the variation of shape fixity ratio as a function of immersing time, Ca^{2+} and Fe^{3+} were chosen as two model metal ions. The shape fixity ratio increases with immersing time as

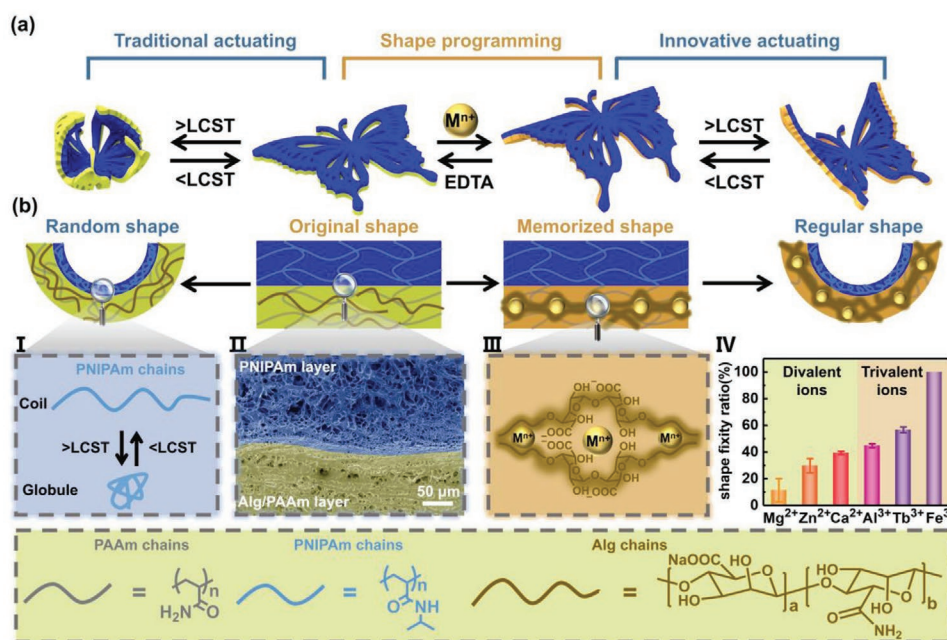


Figure 1. a) Schematic illustration of traditional actuating process triggered by temperature, and programmable shape deformation generated by the combination of shape memory and actuating functions, the wings of butterfly-shaped bilayer hydrogel is first fixed into curved shape by the metal ion-Alg interactions, and then the wings would deform from the into a curved shape to soaring shaped under the stimulus of heat. b) Schematic illustration of mechanism of shape memory and actuating process: I) mechanism of the volume phase transition of PNIPAm chains. II) The cross-section SEM images of bilayer hydrogel. III) Schematic illustration of metal coordination between Alg chains and ions. IV) Variation of shape fixity ratios of the Alg/PAAm-PNIPAm hydrogel stabilized by different metal ions (0.1 M) with immersing time of 2 min.

expected. If the deformed shape is stabilized by Fe^{3+} , the shape fixity ratio reaches 100% in 20 s, while it takes about 240 s to achieve a constant fixity ratio of about 60% if the deformed hydrogel is fixed by Ca^{2+} (Figure 2b). Since the memorizing layer plays a leading role in the shape fixing process, the shape memory behavior is influenced by the thickness ratio between the memorizing layer and the actuating layer. As shown in Figure 2c, when the thickness of the memorizing layer and the actuating layer is 1:0.5 (unit:mm), both of the shape fixity ratios in the presence of Ca^{2+} and Fe^{3+} can reach about 100%, while the shape fixity ratios are much lower with a small thickness ratio of 0.5:1 (unit:mm). These results indicate that the deformed shape can be well fixed by a thick memorizing layer. While when the thickness ratio is consistent, the shape fixity ratio of a bilayer hydrogel with two thin layers (0.5 mm:0.5 mm) is higher than that with two thick layers (1 mm:1 mm), and there is an obvious difference between the shape fixity ratios caused by Ca^{2+} and Fe^{3+} , therefore hydrogel with two thin layers was selected for further experiment. After the shape fixing process, the bilayer hydrogel with a circular temporary shape was immersed into warm water of 60 °C, which is higher than the lower critical solution temperature of PNIPAm, the PNIPAm network would change from hydrophilic to hydrophobic and release part of the bound water, the actuating layer would shrink as a result, and the hydrogel would deform starting from a temporary shape (Figure 2a). The bending angles are calculated and bending toward the memorizing layer was marked

as a negative angle, as shown in Figure 2d, when the temporary shape is stabilized by Ca^{2+} , the shrinkage of the actuating layer would drive the bilayer hydrogel to turn to straight first and then bend to the actuating layer, while only a straight final shape is observed when the temporary shape is fixed by Fe^{3+} .

In order to explore the influence of shape memory on actuating behavior, the moduli and mechanical properties of the memorizing layer in the absence and presence of metal ions were investigated by frequency-sweep rheological and tensile tests, respectively. As shown in Figure S4, Supporting Information, the storage modulus (G') and loss modulus (G'') of the Ca^{2+} treated memorizing layer are higher than that of the untreated sample, and G' and G'' of the two samples are lower than that of the Fe^{3+} treated sample. It is indicated that the hydrogel would become tougher when treated by Ca^{2+} and Fe^{3+} , respectively. The same conclusion can be drawn through tensile tests that the stress of Ca^{2+} treated sample is higher than the untreated sample but lower than the Fe^{3+} treated sample (Figure S5, Supporting Information). It can be deduced that a firm memorizing layer is difficult to be driven by the actuating layer, which results in different actuating degrees. Besides, the actuating velocity is also different when treated with different metal ions (Figure S6, Supporting Information). Furthermore, the shape memory layer would become tougher with increasing shape fixing time (Figure S7, Supporting Information), and the actuating velocity would become slower both in Ca^{2+} treated sample and Fe^{3+} treated sample (Figure S8, Supporting

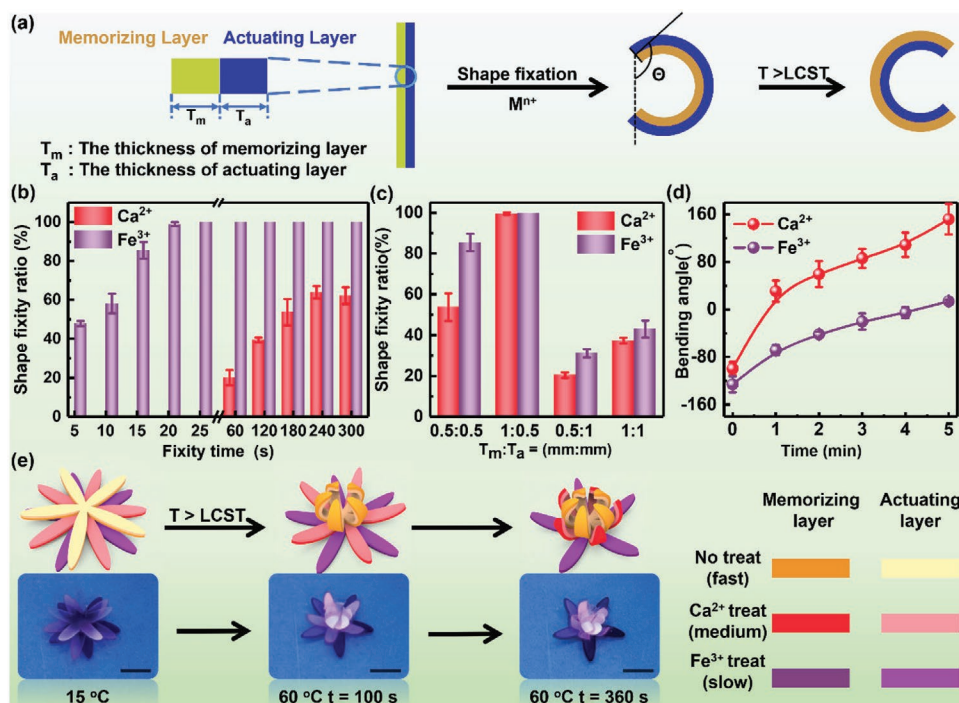


Figure 2. a) Schematic illustration of the shape deformation behavior of a bilayer hydrogel strip. The hydrogel strip is first fixed into a temporary circular shape via the coordination between metal ions and alginate, and then deforms in warm water (60 °C) based on the contraction of the PNIPAm actuating layer. b) Variation of shape fixity ratios of the Alg/PAAm-PNIPAM hydrogel in CaCl_2 or FeCl_3 solution as a function of immersing time. c) Variation of shape fixity ratios of the Alg/PAAm-PNIPAM hydrogel as a function of thickness ratio between memorizing layer and actuating layer in CaCl_2 or FeCl_3 solution. d) Variation of bending angles of the hydrogel strip with a fixed temporary shape by Ca^{2+} or Fe^{3+} in warm water (60 °C). e) The step wise shape deformation process of the biomimetic hydrogel flower (the untreated hydrogel layer is stained with congo red, the Ca^{2+} treated hydrogel is stained with rhodamine B, the Fe^{3+} treated hydrogel is stained with methyl violet). Scale bar: 1 cm.

Information). Therefore, a biomimetic hydrogel flower was prepared to integrate fast actuating (no treated), middle actuating (Ca^{2+} treated), slow actuating (Fe^{3+} treated) performances in one system, as shown Figure 2e, upon the treating of warm water, the hydrogel sequence could close in sequence, realize step wisely shape deformation behavior.

Taking advantage of the shape memory function, a simple hydrogel strip can be fixed into various temporary shapes, and accomplishing diverse shape transformation behaviors under the stimulus of heat. As shown in Figure S8, Supporting Information, a hydrogel strip with a size of $40 \text{ mm} \times 2 \text{ mm} \times (0.5 + 0.5) \text{ mm}$ was patterning treated by Fe^{3+} , the modulus of the treated parts would increase due to the coordination between Fe^{3+} and alginate chains, then the hydrogel strip was transferred into warm water (60°C), the untreated part is easy to be deformed, and the straight hydrogel strip would form 2D shapes such as “6,” “triangle,” and “U.” In addition, when the hydrogel strips were given a 2D temporary shape by Fe^{3+} , such as V-shaped, crutch-shaped (Figure S10, Supporting Information). It is necessary to note that the V-type has two forms with the memorizing layer inside and outside, respectively. Similarly, when the hydrogel strip with 2D temporary shapes are placed in warm water, they would transform into heart, musical note, and “3” shapes, respectively, and the shape transformation is fully reversible if the hydrogel is treated in cold water (Figure S11, Supporting Information).

In general, a straight bilayer hydrogel strip will bend under stimulus due to the shrinkage of one layer, so it can only change from 1D to 2D. By integrating shape memory and actuating, complex shape deformation behaviors can be realized. As shown in Figure 3a and Figure S12, Supporting Information, a 1D hydrogel strip was twisted to the clockwise (top to bottom view) and the shape was fixed after immersing in 0.1 M Ca^{2+} solution for 5 min. With increasing temperature, the twisted hydrogel strip can magically transform from clockwise twisted shape (1D) to right-handed spiral shape (3D) directly, which has never been reported before. Similarly, if the hydrogel strip was fixed into a counterclockwise twist shape, it will actuate into left-handed spiral shape. Besides the hydrogel could be restored from 3D spiral state to 1D twist state in cold water at 15°C , and it would finally restore to the 1D straight state after being treated with 0.1 M EDTA , thereby the transformation from 1D to 3D to 1D is realized (Figure S13, Supporting Information).

In order to better elaborate the process of the shape deformation, the head of the twisted hydrogel strip was anchored while the tail was marked. The shape deformation process was observed from both horizontal and vertical directions, and the motion track of the tail of twisted hydrogel strip was recorded (Figure 3b). It is indicated when the straight hydrogel strip was fixed into twisted shape, the hydrogel exhibited anisotropic structure both in horizontal and vertical direction while the original hydrogel only exhibited anisotropic in horizontal direction. Therefore, the horizontal and vertical shrink

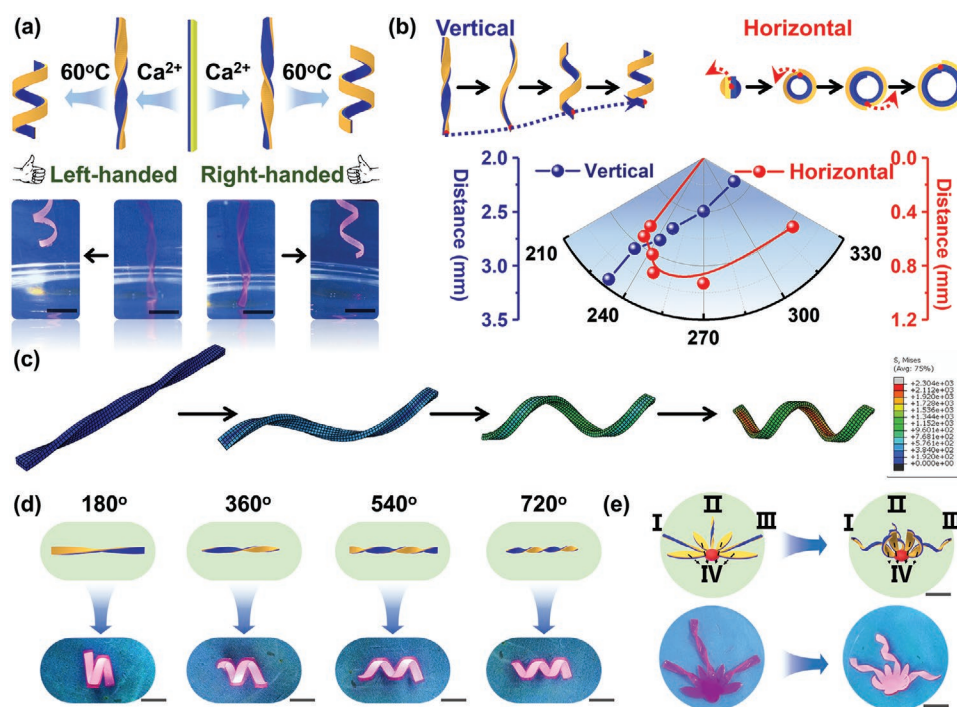


Figure 3. a) Illustration and images showing the deformation of hydrogel strip from 1D straight state to 1D twisted state by shape memory, and then transform to 3D spiral state by actuation. b) Schematic representation and polar plot showing the trajectory and trend of the hydrogel during the actuating process. c) Finite element modeling of the shape transformation from clockwise twist to right-handed spiral. d) The shape deformation behaviors of a bilayer hydrogel strip after being fixed into right helix with different twisted angle. e) Illustration and images showing the biomimetic shape transformation of a hydrogel orchid (type I: the hydrogel strip was twisted left with 180° and transform into a left spiral, type II: the hydrogel strip was twisted left with 360° and transform into a left spiral, type III: the hydrogel strip was twisted right with 180° and transform into a right spiral, type IV: the hydrogel sheet is bent after deformation). Scale bar: 1 cm.

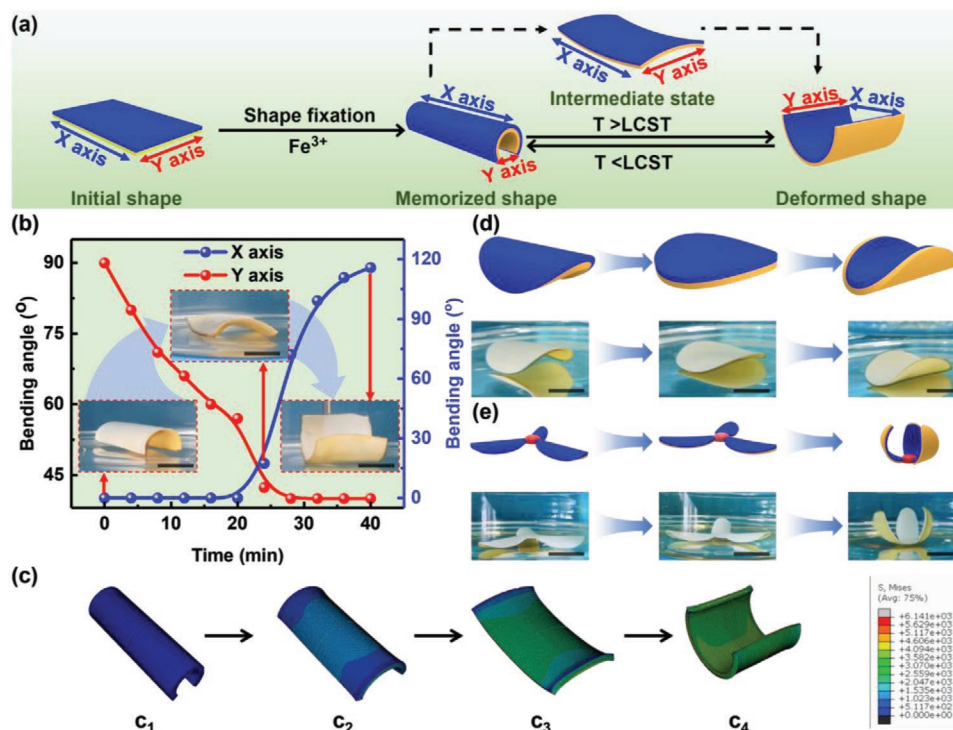


Figure 4. a) Schematic representation and b) digital and images showing the process of 3D shapes transition of a rectangular bilayer hydrogel sheet. c) Finite element modeling of the actuating process of a rectangular bilayer hydrogel sheet. 3D shape transition images of d) circular and e) flower shape hydrogel sheet. Scale bar: 1 cm.

process synergistically leads the shape deformation from strip to spiral. The shape deformation behavior was simulated by finite element modeling and the results are highly consistent with the experimental results (Figure 3c). Due to the programmable shape memory function, various temporary anisotropic structure could be generated such as clockwise-counterclockwise twist shape, different twist degree shape with 180°, 360°, 540°, 720°, leading to diverse corresponding complex shape deformation behaviors (Figure 3d and Figure S14, Supporting Information). The reprogrammable actuating behaviors encourage us to explore the biomimetic performances of the bilayer hydrogel, as shown in Figure 3e, we have imitated the complex shape deformation of orchid *Dendrobium helix* by the assisting of shape memory property. A hydrogel orchid has been fabricated, and the petals were twisted and stabilized with metal ions, and the hydrogel orchid could deform in warm water and resemble the 3D morphology of orchid and exhibits three types of shape transformation (right-handed spiral, left-handed spiral, and bending).

Besides bilayer hydrogel strip, fascinating shape transformation behaviors could be realized by bilayer hydrogel sheet due to the synergy between shape memory and actuation performances. As shown in Figure 4a, a rectangular hydrogel sheet was fixed into a temporary tubular structure toward the memorizing side along the *x*-axis by Fe³⁺, when placed into warm water, the hydrogel sheet first unrolled to form a flat intermediate state and then bent toward the actuating side along the *y*-axis due to the shrinkage of the actuating layer. During this process, the *x*-axis of hydrogel tube cannot bend at the beginning because of the restriction of the 3D fixed shape. So, the

contraction of the actuating side first generated stress to unfold the hydrogel sheet. With the transformation from cylinder to flat, the *x*-axis constraint force caused by the cylindrical structure was eliminated, then the cumulative contraction stress along the *x*-axis can be released and drove the hydrogel sheet turn into an arched structure in the opposite direction along the *y*-axis. The bending angle of the *y*-axis decreases about from 90° to 40° first, then the bending angle of the *x*-axis increases from about 0° to 120° (Figure 4b). The shape deformation behavior is highly consistent with the deformation process predicted by Finite element modeling (Figure 4c). Similar actuating behaviors have been witnessed by the above hydrogel sheet which was memorized along the *x*-axis, a circular hydrogel sheet, and a triangular hydrogel sheet (Figure 4d; Figures S15 and S16, Supporting Information). Finally, a hydrogel flower with three petals was constructed, and the petals were bent to the lower side (memorizing side) and fixed at first, upon immersed in warm water, the petals turned to flat and then bent to the upper side (actuating side) to form a blooming flower (Figure 4e).

With the assistance of kirigami, complex shape transformation behaviors could be achieved. As shown in Figure 5a, a square bilayer hydrogel sheet was cut deliberately, then the hydrogel sheet was rolled into cylinders and both ends of it were treated by Fe³⁺, and the cylinder shape was thus fixed (Figure 5b₁,b₂). When the hydrogel cylinder was immersing into warm water, the central part of it would deform, and the hydrogel cylinder could evolve into a lantern (Figure 5b₃,b₄). Moreover, the lantern shape could be accomplished from an entirely different way (Figure 5c). The 2D hydrogel sheet could be deformed and fixed into an arched shape by treating the

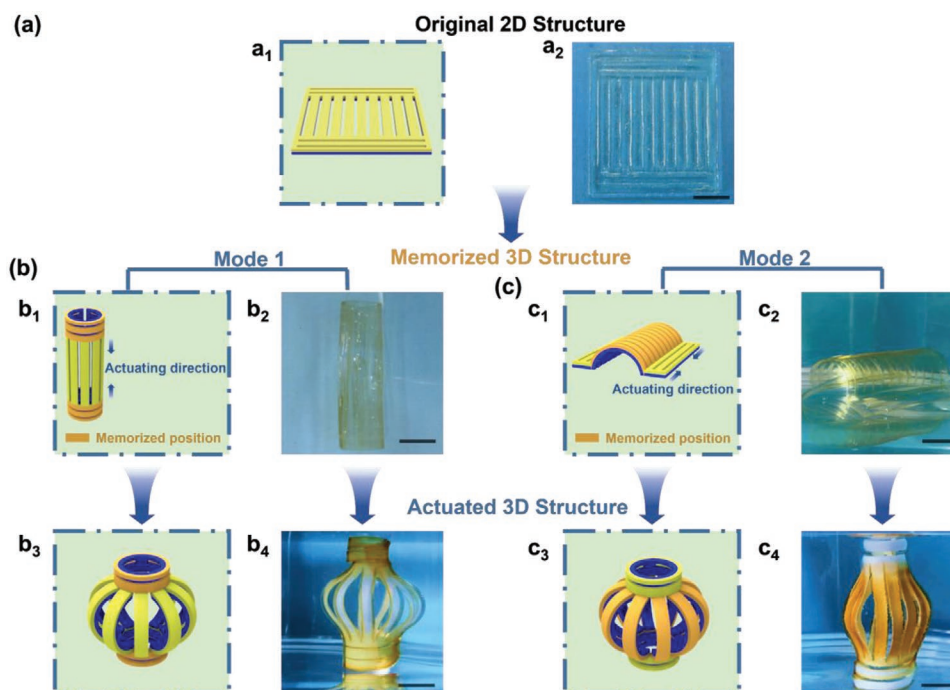


Figure 5. a) With the assistance of kirigami, a bilayer hydrogels sheet with cut patterns can be first fixed into a b) cylinder or c) an arched shape, and both of them could evolve into lantern shapes by immersing into warm water (60 °C). The inset orange patterns of b₁, b₃, c₁, and c₃ represent these areas are treated by Fe³⁺. Scale bar: 1 cm.

arched part with Fe³⁺ (Figure 5c_{1,c2}), both ends of the arched shape could actuate into a circle with increasing temperature, and a lantern shape was thus achieved (Figure 5c_{3,c4}).

3. Conclusion

In conclusion, a bilayer hydrogel which is composed of Alg/PAAm as the memorizing layer and PNIPAm as the thermoresponsive actuating layer has been fabricated. Various temporary shapes can be stabilized through the coordination between alginate and metal ions, then the hydrogel could reversibly actuate from the programmable temporary shape caused by the shrinkage of PNIPAm layer under the trigger of heat. Both the shape fixity ratio and actuating behaviors could be regulated by choosing different metal ions to realize sequentially shape deformation behavior. Taking advantage of shape memory function, diverse anisotropic structures could be formed from one initial hydrogel, and achieving various complex shape deformation behaviors. Moreover, complex shape transformation behaviors could be accomplished with the assistance of kirigami. In conclusion, the strategy of actuating supramolecular shape memorized hydrogel could be used to achieve programmable shape deformation for a better biomimetic of actuation behavior in nature. We believe our strategy would provide innovative ideas for the design and fabrication of bioactuators.

Supporting Information

Supporting Information is available from the Wiley Online Library or from the author.

Acknowledgements

This work was supported by National Natural Science Foundation of China (51873223, 52073295), the National Key Research and Development Program of China (2018YFB1105100, 2019YFC1606600, and 2019YFC1606603), Youth Innovation Promotion Association of Chinese Academy of Sciences (2017337, 2019297), Key Research Program of Frontier Science, Chinese Academy of Sciences (QYZDB-SSW-SLH036), K. C. Wong Education Foundation (CJTD-2019-13).

Conflict of Interest

The authors declare no conflict of interest.

Keywords

actuating, bilayer hydrogel, programmable shape deformation, shape memory

Received: September 3, 2020
Revised: October 4, 2020
Published online: November 9, 2020

- [1] Z. Z. Zhao, R. C. Feng, Q. F. Rong, M. J. Liu, *Adv. Mater.* **2017**, *29*, 1703045.
- [2] L. R. Shang, W. X. Zhang, K. Xu, Y. J. Zhao, *Mater. Horiz.* **2019**, *6*, 945.
- [3] H. L. Fan, J. P. Gong, *Macromolecules* **2020**, *53*, 2769.
- [4] T. Matsuda, R. Kawakami, R. Namba, T. Nakajima, J. P. Gong, *Science* **2019**, *363*, 504.

- [5] D. L. Gan, W. S. Xing, L. L. Jiang, J. Fang, C. C. Zhao, F. Z. Ren, L. M. Fang, K. F. Wang, X. Lu, *Nat. Commun.* **2019**, *10*, 1487.
- [6] R. Kempaiah, Z. H. Nie, *J. Mater. Chem. B* **2014**, *2*, 2357.
- [7] X. X. Le, W. Lu, J. W. Zhang, T. Chen, *Adv. Sci.* **2019**, *6*, 1801584.
- [8] H. L. Cui, N. Pan, W. X. Fan, C. Z. Liu, Y. Z. Xia, K. Y. Sui, *Adv. Funct. Mater.* **2019**, *29*, 1807692.
- [9] Y. S. Zhao, C. Xuan, X. S. Qian, Y. Alsaïd, M. Hua, L. H. Jin, X. M. He, *Sci. Rob.* **2019**, *4*, eaax7112.
- [10] Y. Cheng, K. H. Chan, X. Q. Wang, T. P. Ding, T. T. Li, X. Lu, G. W. Ho, *ACS Nano* **2019**, *13*, 13176.
- [11] G. P. Chen, Y. R. Yu, X. W. Wu, G. F. Wang, J. N. Ren, Y. J. Zhao, *Adv. Funct. Mater.* **2018**, *28*, 1801386.
- [12] F. Y. Li, D. Lyu, S. Liu, W. W. Guo, *Adv. Mater.* **2020**, *32*, 1806538.
- [13] S. X. Wei, W. Lu, X. X. Le, C. X. Ma, H. Lin, B. Y. Wu, J. W. Zhang, P. Theato, T. Chen, *Angew. Chem., Int. Ed.* **2019**, *58*, 16243.
- [14] W. X. Fan, C. Y. Shan, H. Y. Guo, J. W. Sang, R. Wang, R. R. Zheng, K. Y. Sui, Z. H. Nie, *Sci. Adv.* **2019**, *5*, eaav7174.
- [15] Y. Tan, D. Wang, H. X. Xu, Y. Yang, X. L. Wang, F. Tian, P. P. Xu, W. L. An, X. Zhao, S. M. Xu, *ACS Appl. Mater. Interfaces* **2018**, *10*, 40125.
- [16] X. M. He, Y. Sun, J. H. Wu, Y. Wang, F. Chen, P. Fan, M. Q. Zhong, S. W. Xiao, D. Zhang, J. T. Yang, J. Zheng, *J. Mater. Chem. C* **2019**, *7*, 4970.
- [17] C. X. Ma, T. F. Li, Q. Zhao, X. X. Yang, J. J. Wu, Y. W. Luo, T. Xie, *Adv. Mater.* **2014**, *26*, 5665.
- [18] A. Cangialosi, C. Yoon, J. Y. Liu, Q. Huang, J. K. Guo, T. D. Nguyen, D. H. Gracias, R. Schulman, *Science* **2017**, *357*, 1126.
- [19] X. P. Hao, Z. Xu, C. Yu, W. Hong, Q. Zheng, Z. L. Wu, *Adv. Mater.* **2020**, *32*, 2000781.
- [20] A. Nojoomi, H. Arslan, K. Lee, K. Yum, *Nat. Commun.* **2018**, *9*, 3705.
- [21] M. J. Liu, Y. Ishida, Y. Ebina, T. Sasaki, T. Hikima, M. Takata, T. Aida, *Nature* **2015**, *517*, 68.
- [22] Y. Yang, Y. Tan, X. L. Wang, W. L. An, S. M. Xu, W. Liao, Y. Z. Wang, *ACS Appl. Mater. Interfaces* **2018**, *10*, 7688.
- [23] Z. L. Wu, M. Moshe, J. Greener, H. T. Aubin, Z. H. Nie, E. Sharon, E. Kumacheva, *Nat. Commun.* **2013**, *4*, 1586.
- [24] A. M. Abdullah, X. L. Li, P. V. Braun, J. A. Rogers, K. J. Hsia, *Adv. Mater.* **2018**, *30*, 1801669.
- [25] H. Arslan, A. Nojoomi, J. H. Jeon, K. Yum, *Adv. Sci.* **2019**, *6*, 1800703.
- [26] L. M. Huang, R. Q. Jiang, J. J. Wu, J. Z. Song, H. Bai, B. Li, Q. Zhao, T. Xie, *Adv. Mater.* **2017**, *29*, 1605390.
- [27] A. S. Gladman, E. A. Matsumoto, R. G. Nuzzo, L. Mahadevan, J. A. Lewis, *Nat. Mater.* **2016**, *15*, 413.
- [28] J. H. Guo, R. R. Zhang, L. N. Zhang, *ACS Macro Lett.* **2018**, *7*, 442.
- [29] Y. L. Hu, Z. Y. Wang, D. D. Jin, C. C. Zhang, R. Sun, Z. Q. Li, K. Hu, J. C. Ni, Z. Cai, D. Pan, X. W. Wang, W. L. Zhu, J. W. Li, D. Wu, L. Zhang, J. R. Chu, *Adv. Funct. Mater.* **2020**, *30*, 1907377.
- [30] W. J. Peng, G. G. Zhang, J. Liu, S. Nie, Y. Wu, S. H. Deng, G. Q. Fang, J. Zhou, J. Z. Song, J. Qian, P. J. Pan, Q. Zhao, T. Xie, *Adv. Funct. Mater.* **2020**, *30*, 2000522.
- [31] M. Vázquez-González, I. Willner, *Angew. Chem., Int. Ed.* **2020**, *59*, 15342.
- [32] W. Lu, X. X. Le, J. W. Zhang, Y. J. Huang, T. Chen, *Chem. Soc. Rev.* **2017**, *46*, 1284.
- [33] X. Li, M. J. Serpe, *Adv. Funct. Mater.* **2016**, *26*, 3282.
- [34] Z. Jiang, B. Diggle, I. C. G. Shackelford, L. A. Connal, *Adv. Mater.* **2019**, *31*, 1904956.
- [35] Z. Y. Li, G. Davidson-Rozenfeld, M. Vázquez-González, M. Fadeev, J. J. Zhang, H. Tian, I. Willner, *J. Am. Chem. Soc.* **2018**, *140*, 17691.
- [36] A. Yasin, W. F. Zhou, H. Y. Yang, H. Z. Li, Y. Chen, X. Y. Zhang, *Macromol. Rapid Commun.* **2015**, *36*, 845.
- [37] Z. G. Zhao, S. Y. Zhuo, R. C. Fang, L. H. Zhang, X. T. Zhou, Y. C. Xu, J. Q. Zhang, Z. C. Dong, L. Jiang, M. J. Liu, *Adv. Mater.* **2018**, *30*, 1804435.
- [38] T. Z. Li, J. H. Wang, L. Y. Zhang, J. B. Yang, M. Y. Yang, D. Y. Zhu, X. H. Zhou, S. H. Wang, Y. Z. Liu, X. C. Zhou, *J. Mater. Chem. B* **2017**, *5*, 5726.
- [39] J. Y. Sun, X. H. Zhao, W. R. K. Illeperuma, O. Chaudhuri, K. H. Oh, D. J. Mooney, J. J. Vlassak, Z. G. Suo, *Nature* **2012**, *489*, 133.
- [40] S. W. Xiao, M. Z. Zhang, X. M. He, L. Huang, Y. X. Zhang, B. P. Ren, M. Q. Zhong, Y. Chang, J. T. Yang, J. Zheng, *ACS Appl. Mater. Interfaces* **2018**, *10*, 21642.